MODEL FOR DOPPLER RADAR RADIAL WINDS

Kirsti Salonen[1],[*] Heikki Järvinen[1], Magnus Lindskog[2]
1. Finnish Meteorological Institute, 2. Swedish Meteorological and Hydrological Institute

1. INTRODUCTION

Interpretation of radar measurements is usually obtained through geophysical inversion, such as Z-R relationship or VAD technique. An alternative method to interpret and to quantitatively exploit radar measurements is data assimilation. It consists of modelling the radar measurement with the Numerical Weather Prediction (NWP) model variables. In data assimilation, the difference between the model counterpart and the observation is minimized. The solution is constrained by the NWP model background and by all available observational information and thus the problem is nearly always well-posed, unlike the geophysical inversion. Data assimilation enables exploitation of a wide variety of indirect observations of the NWP model variables through observation modelling. In this article we describe the observation modelling for the Doppler radar radial winds.

Our work with Doppler radar radial wind data is part of the research and co-operation within European Union COST 717 action concerning 'Use of Radar Observations in Hydrological and NWP models (Rossa, 2000).

Section 2. of this article describes the characteristics of Doppler radar radial wind superobservations. Formulation of the observation operator is provided in Section 3. Some test results are given in Section 4. and the article is concluded by a brief summary in Section 5.

2. DOPPLER RADAR RADIAL WIND SUPEROBSERVATIONS

Doppler radars produce radial wind raw data with high temporal and spatial density. The horizontal resolution of this data is around one kilometer whereas the typical resolution of a mesoscale NWP model is of the order of ten kilometers. Doppler radar wind observations thus represent partly phenomena which are not resolved by the NWP model. Calculating spatial averages from the raw data, called superobservations (SO), decreases this representativeness error. The processing software for SO generation has been developed as an extension to

[*] *Corresponding author address*: Kirsti Salonen, Finnish Meteorological Institute, P.O.BOX 503, FIN-00101 Helsinki, Finland; e-mail: kirsti.salonen@fmi.fi
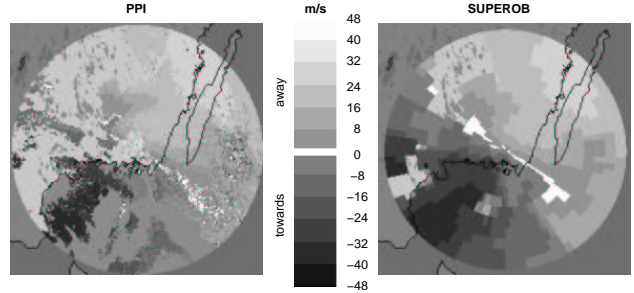
Figure 1: An example of the Doppler radar radial wind raw data (left) and superobservations generated through horizontal averaging (right)

the Radar Analysis and Visualization Environment RAVE (Michelson, 1999).

Figure 1 displays the radial wind raw data and the corresponding SO with a scale of approximately 10 km. If the horizontal scale of the SO would be further increased, radial winds with significantly different measurement directions would be averaged close to the radar, and that is not desirable.

3. OBSERVATION OPERATOR

Three dimensional variational data assimilation (3D-Var) is based on the minimization of the cost function

$$
\begin{aligned}
J &= J_b + J_o = \frac{1}{2}(\mathbf{x} - \mathbf{x^b})^{\mathbf{T}}\mathbf{B}^{-1}(\mathbf{x} - \mathbf{x^b}) \\
&+ \frac{1}{2}(\mathbf{y} - H\mathbf{x})^{\mathbf{T}}\mathbf{R}^{-1}(\mathbf{y} - H\mathbf{x}),
\end{aligned}
\tag{1}
$$

where J_b measures the distance of the model state vector $\mathbf{x}$ to the model background state vector $\mathbf{x^b}$ and J_o measures the distance to the observation vector $\mathbf{y}$, respectively (Gustafsson et al. 2001). Observation operator H produces the model counterpart of the observed quantity.

3.1 The standard observation operator

The formulation of the standard observation operator for the Doppler radar radial winds (Lindskog et al. 2000) involves

1. Bi-linear interpolation of the NWP model horizontal wind components u and v to the observation location.

2. Projection of the interpolated NWP model horizontal wind towards the radar

$$v_h = u \sin \theta + v \cos \theta, \qquad (2)$$

where θ is the azimuth angle of the radar beam.

3. Projection of v_h in (2) on the slanted direction of the radar beam

$$
\begin{aligned}
v_r &= v_h \cos(\phi + \alpha), \\
\alpha &= \arctan\left(\frac{d \cos \phi}{d \sin \phi + r + h}\right), \qquad (3)
\end{aligned}
$$

where ϕ is the elevation angle of the radar beam, d is the measurement range, r is the radius of the Earth and h is the height of the radar above the mean sea level. The formula for α takes approximately into account the curvature of the Earth. The observing geometry of the projection is illustrated in Fig. 2.

It is assumed in this standard formulation of the observation operator that there is no mean velocity towards the radar due to precipitation. This implicit assumption is embedded into (2) where only the NWP model horizontal wind is included. This assumption is justified for assimilation of Doppler radar radial wind measurements with low elevation angles.

3.2 Modelling the broadening of the radar beam

The standard formulation of the Doppler radar radial wind observation operator does not account for the radar beam broadening. This assumption is relaxed in this section by appropriate modelling.

The shape of the radar beam main lobe is approximately Gaussian (Probert-Jones 1962). This provides an elementary approach to model the broadening of the radar beam in the observation operator. We introduce a Gaussian averaging kernel for the vertical interpolation of the NWP model horizontal wind components (u and v in (2)) to the observation location. In the standard formulation a linear interpolation is applied in the vertical. The Gaussian averaging kernel reads

$$
\begin{aligned}
w &= \frac{1}{2\pi} \exp\left(-\frac{(z - z_0)^2}{\kappa}\right), \\
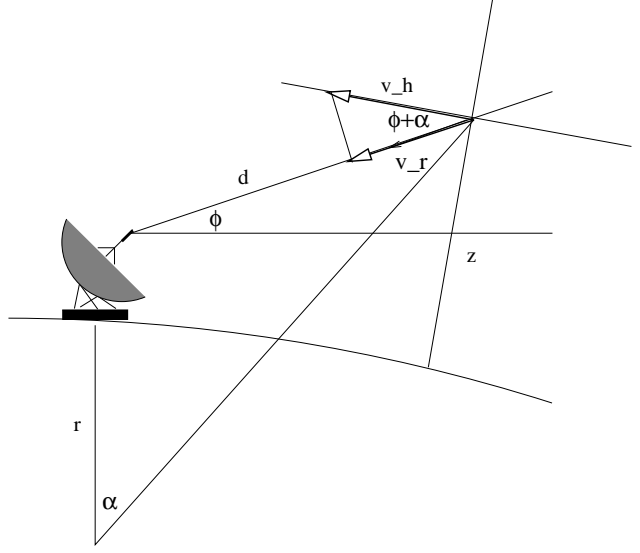\kappa &= (z_k - z_0)^2, \qquad (4)
\end{aligned}
$$

Figure 2: The geometry of calculating the NWP model counterpart of the Doppler radar radial wind. r is the Earth's radius, d the measurement range, ϕ the elevation angle and α approximates the curvature of the Earth.

where z is the model level height and z_0 the observation height. κ defines the width of the kernel, where z_k is the height of the upper limit of half-power beamwidth calculated with $\frac{4}{3}$r -law at the measurement distance d. Fig. 3 displays the beam broadening and examples of the vertical averaging kernel at ranges of 50 km and 150 km.

An unwanted feature with the choice of the Gaussian averaging kernel is that the kernel is non-zero from the Earth's surface to the top of the atmosphere. Consequently, the model counterpart would consist of the NWP model wind values of the whole model wind profile at the measurement location. Of course, only the wind information which the radar is able to measure should be included into the model counterpart. Two limitations are therefore included into the vertical averaging kernel:

1. Radar is unable to see below the radar horizon. The obscuring effect of the radar horizon is taken into account by assuming a radar horizon of $0°$ elevation angle, below which the model information is not used. This lower limit of the averaging kernel is denoted by the lower limit of the shaded region in Fig. 3.

2. The observation operator with a Gaussian averaging kernel implicitly assumes a homogeneous field of scatterers between the radar horizon and the top of the model domain. An empirical upper limit is set to 1.5 times the beamwidth (Jarmo Koisti-
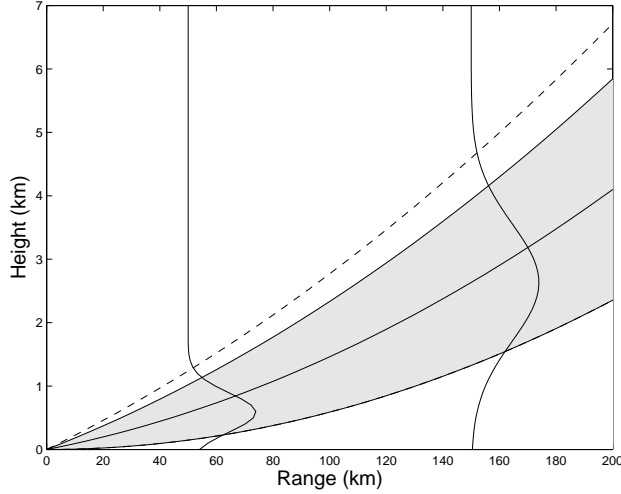
Figure 3: An illustration of the radar beam broadening with 1° beamwidth (shaded area), upper limit for the Gaussian averaging kernel (dashed line) and shapes of the averaging kernel at measurement ranges of 50 km and 150 km. The radar beam elevation angle is 0.5°.

nen, personal communication). This is based on the fact that the upper part of the Gaussian radar beam is located, in most cases (at least at longer ranges and with higher elevation angles), above the scattering hydrometeors or in a region where the radar reflectivity factor is several orders of magnitude smaller than in the lower parts of the beam. Hence upper part of the beam will not significantly contribute to the measured beam-weighted reflectivity or Doppler winds. The upper limit for the averaging kernel is denoted by a dashed line in Fig. 3.

3.3 Modelling the bending of the radar beam

The standard formulation of the Doppler radar radial wind observation operator does not account for the bending of the radar beam. This assumption is relaxed by modelling.

Radar beam bending can be calculated by the Snell's law. Fig. 4 illustrates the radar beam path accross the model levels. The local refraction index can be calculated from the NWP model temperature, pressure and humidity profiles for model levels assuming the refraction index being representative both at the measurement and the radar locations. Refraction index n_{f1} on model full level f_1 represents the refraction index between the model half levels h_1 and h_2. Modified elevation angle ϕ_{h2} can then
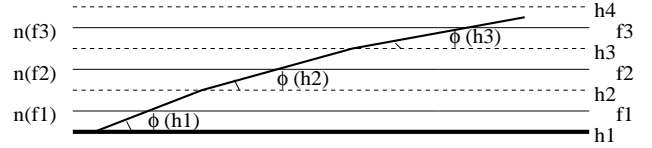

Figure 4: An illustration of the bending of the radar beam in the model atmosphere. Model full levels are displayed with solid lines and model half levels with dashed lines. ϕ is the radar elevation angle, n(f) the refraction index at model full level.

be calculated by

$$\frac{\sin(90 - \phi_{h1})}{\sin(90 - \phi_{h2})} = \frac{n_{f2}}{n_{f1}}. \tag{5}$$

The total bending of radar beam path across the levels $f_1, f_2, \cdots, f_N$ is accumulated in the observation operator until the radar beam reaches the observation location. The last calculated elevation angle is then used in (3) as an *effective elevation angle* when projecting the horizontal wind v_h on the slanted direction of the radar beam. This modifies also the observation height from the value obtained by applying $\frac{4}{3}r$ -law at range d.

4. TEST RESULTS

A 14 day (1-14 June 1999) assimilation experiment has been performed to study the fit of the SO winds with the model background. The observations are from the SMHI radar network with an unambiguous velocity interval of ±48 m/s. The model counterpart is calculated from the model background state $\mathbf{x}^b$, which is a 6-hour forecast of the FMI operational HIRLAM NWP system. The horizontal resolution of the model is 0.4°. Two alternative NWP model vertical resolutions are used in the experiments (31 and 40 levels).

A number of supporting variables are derived as a by-product of SO generation. These can be used as quality criteria for SO data, which should be representative for the whole averaging area, not only for one polar bin. The assimilation experiment indicates that an SO should be rejected if it consists of less than 5 polar bin raw data elements or if its variance is larger than 10 m^2/s^2. The maximum measurement range is limited to 100 km. These quality criteria are applied in the experiments.

Data assimilation experiments provide statistical material to study the fit of SO to the NWP model counterpart. First, the sensitivity of this fit to the NWP model vertical resolution is studied. Figure 5 displays the mean and rms difference between SO and model counterpart for the standard observation operator using 31 (dash-dotted line)

and 40 vertical levels (solid line) in the NWP model. Both the mean and the rms difference are sensitive for the vertical resolution. With 40 NWP model vertical levels, the model radial wind is slower than the observed wind. With 31 NWP model vertical levels, the opposite is true. In both cases the mean difference is small up to a range of 25 km. At longer ranges it increases to approximately 0.4 m/s (40 level model) and -0.7 m/s (31 level model). It can be concluded that at longer ranges the 40 level model performs better.

Second, the impact of modelling the vertical radar beam broadening is studied. Mean and rms difference for the observation operator using Gaussian averaging kernel is shown in Fig. 5 (dashed line). It can be concluded that the impact of applying the Gaussian averaging kernel in the observation operator is fairly small in these experiments. The mean difference at longer ranges (over 60 km) and the rms difference are slightly better with the modified observation operator. It should be kept in mind, however, that the choice of κ in (4) is *ad hoc* and the effect of varying κ needs to be further studied.

The effect of accounting for the radar beam bending is of the order of $\pm 10^{-4}$ m/s on the mean and rms difference (not shown). This can be understood by studying (3). In normal atmospheric conditions (ICAO atmosphere) with the radar elevation angle of $1.5°$ at two kilometers altitude, the effective elevation angle derived from (5) is $1.3°$. As a result, $\cos(\phi + \alpha)$ of (3) changes by a factor of 10^{-4}.

5. SUMMARY

Observation operator for Doppler radar radial winds has been developed and tested for HIRLAM 3D-Var assimilation system. Assimilation experiments revealed that the mean and rms difference between the observed wind and model counterpart is sensible for the vertical resolution of the model. The 40 level model gives better results at measurement ranges over 40 km.

The improved observation operator takes into account the broadening of the radar beam by applying a Gaussian vertical averaging kernel, and the bending of the radar beam by applying Snell's law. The impact of these improvements is quite small on mean and rms difference. The effect of varying the value of κ in the averaging kernel will be further studied.

REFERENCES

Doviak, R. J. and D. S. Zrnic, 1993: Doppler radar and weather observations. Second edition. *San Diego Academic Press, Inc., 562 pp.*
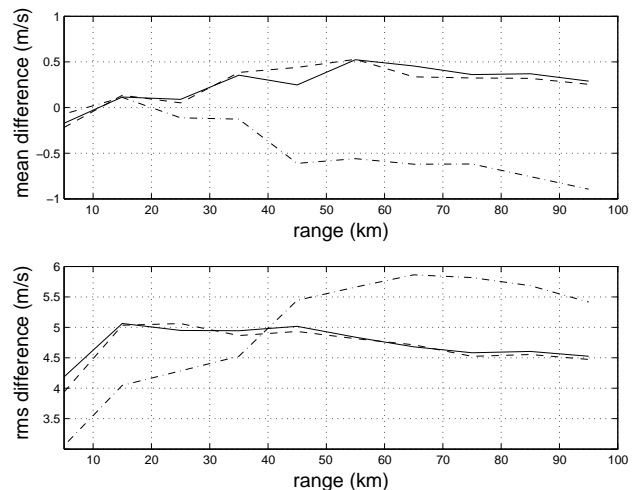
Figure 5: Mean (upper panel) and rms difference (lower panel) between the SO and the model counterpart as a function of range. The standard observation operator and 40 (31) vertical levels in the NWP model is denoted by solid line (dash-dotted line). The observation operator with Gaussian averaging kernel and 40 levels is denoted by dashed line.

Gustafsson, N., Berre, L., Hörnquist, S., Huang, X.-Y., Lindskog, M., Navascués, B., Mogensen, K.S., and Thorsteinsson, S., 2001: Three-dimensional variational data assimilation for a limited area model. Part I: General formulation and the background error constraint. *Tellus*, **53A**, No. 4, 425-446.

Lindskog, M., Järvinen, H. and Michelson, D. B., 2000: Assimilation of Radar Radial Winds in the HIRLAM 3D-Var. *Phys. Chem. Earth (B)*, **25**, No. 10-12, 1243-1249.

Michelson, D B, 1999: RAVE User's Guide. *Available from SMHI, SE-601 76, Norrköping, Sweden. 51 pp.*.

Probert-Jones, J. R., 1962: The radar equation in meteorology. *Quart. J. Roy. Meteor. Soc.*, **88**, 485-495.

Rossa, A., 2000: COST-717: Use of Radar Observations in Hydrological and NWP Models. *Phys. Chem. Earth (B)*, **25**, No. 10-12, 1221-1224.